Research Article

An autonomously self-assembling dendritic DNA nanostructure for target DNA detection

Harish Chandran[1], Abhijit Rangnekar[2], Geetha Shetty[3], Erik A. Schultes[4], John H. Reif[1] and Thomas H. LaBean[2]

[1] Department of Computer Science, Duke University, Durham, NC, USA
[2] Department of Materials Science and Engineering, North Carolina State University, Raleigh, NC, USA
[3] Institute for Regenerative Medicine, Texas A&M Health Science Center, College of Medicine at Scott & White, Temple, TX, USA
[4] Leiden University Medical Center, Leiden, The Netherlands

There is a growing need for sensitive and reliable nucleic acid detection methods that are convenient and inexpensive. Responsive and programmable DNA nanostructures have shown great promise as chemical detection systems. Here, we describe a DNA detection system employing the triggered self-assembly of a novel DNA dendritic nanostructure. The detection protocol is executed autonomously without external intervention. Detection begins when a specific, single-stranded target DNA strand (T) triggers a hybridization chain reaction (HCR) between two, distinct DNA hairpins (α and β). Each hairpin opens and hybridizes up to two copies of the other. In the absence of T, α and β are stable and remain in their poised, closed-hairpin form. In the presence of T, α hairpins are opened by toe-hold mediated strand-displacement, each of which then opens and hybridizes two β hairpins. Likewise, each opened β hairpin can open and hybridize two α hairpins. Hence, each layer of the growing dendritic nanostructure can in principle accommodate an exponentially increasing number of cognate molecules, generating a high molecular weight nanostructure. This HCR system has minimal sequence constraints, allowing reconfiguration for the detection of arbitrary target sequences. Here, we demonstrate detection of unique sequence identifiers of HIV and *Chlamydia* pathogens.

Received	25 APR 2012
Revised	09 AUG 2012
Accepted	06 SEP 2012
Accepted article online	11 SEP 2012

Supporting information available online

Keywords: DNA sequence detection · Hybridization cascade · Molecular self-assembly · Nanobiotechnology · Nucleic acids

1 Introduction

1.1 Hybridization cascades

Strand displacement plays a very important role in DNA nanotechnology. It was first demonstrated by Yurke et al. [1] that a DNA strand with a toe-hold (unpaired nucleotides at the end of the strand) can be extracted from a duplex by binding the strand's full complement to it. Since then, this characteristic has been exploited in various applications such as DNA machines [2], gears [3], walkers [4, 5], and catalytic DNA circuits [5, 6]. The triggered hybridization chain reaction (HCR), first described by Dirks and Pierce [7], is based on the similar principle and involves a cascade of Watson–Crick mediated, DNA–DNA hybridization events between two distinct hairpin sequences. Each hairpin opens the other via a toe-hold mediated strand displacement [8], resulting in the self-assembly of a nicked DNA double helix from many short DNAs. The hairpin precursors of the HCR are metastable, and can coexist as a mixture of separate molecules, until triggered by the addition of a DNA strand

Correspondence: Prof. Thomas H. LaBean, Department of Materials Science & Engineering, North Carolina State University, EB I Room 3030, 911 Partners Way, Raleigh, NC 27606, USA
E-mail: thlabean@ncsu.edu

Abbreviations: Ct, *Chlamydia trachomatis*; **HCR**, hybridization chain reaction; **HIV**, human immunodeficiency virus; **PAGE**, polyacrylamide gel electrophoresis

Color online: See the article online to view the figures in color.

Biotechnol. J. 2013, 8, 221–227

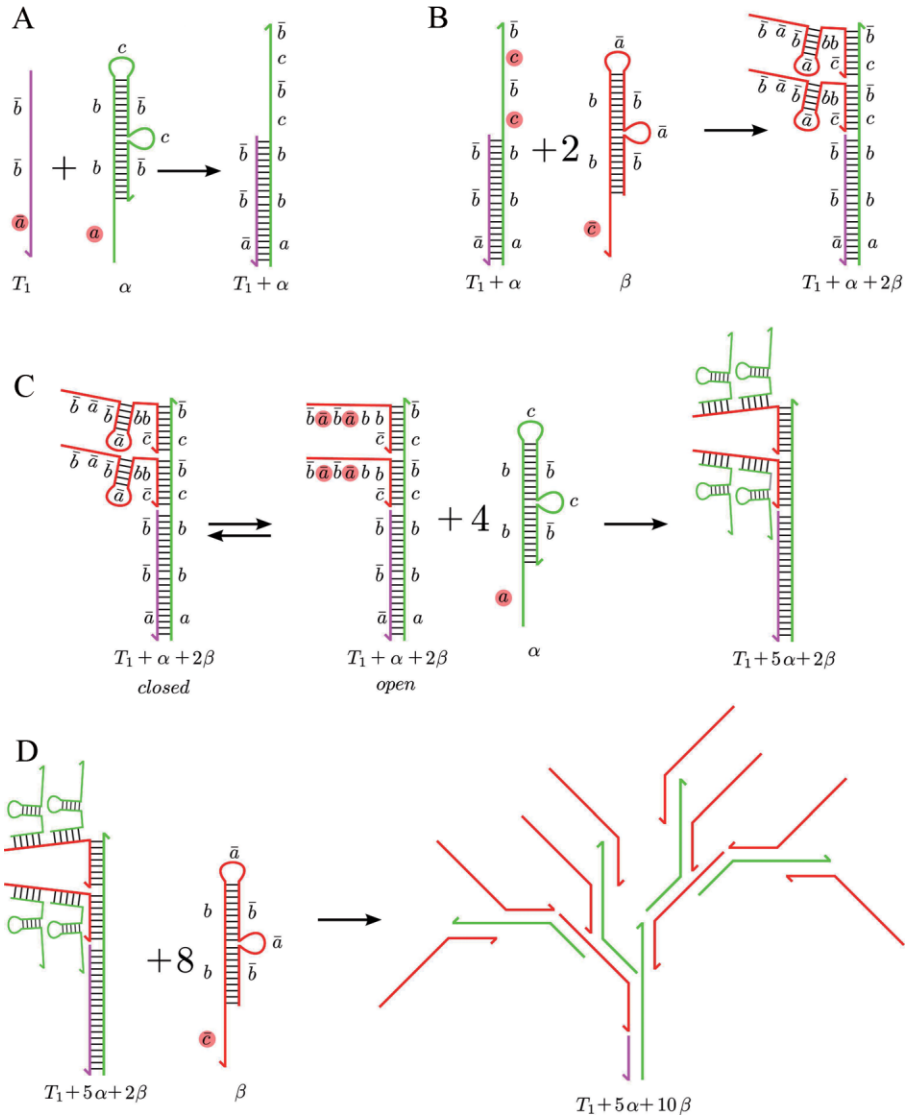

Figure 1. Schematic illustration of dendritic nanostructure formation upon target (T_1) detection. (**A**) Target strand T_1 binds to and opens hairpin α. (**B**) Two copies of hairpin β then bind to T_1 + α complex. (**C**) Opening and closing of stem-loop structure in bound β affect the overall rate of dendrimer formation. Opened form paves the way for the binding of four copies of α constituting the next layer in the dendrimer formation. (**D**) The number of hairpins added to the growing structure at each stage increases exponentially and leads to the dendrimer formation. Here, subsequence a is complementary to subsequence $\bar{a}$ (and so on).

that initiates the opening of at least one of the two hairpin strands.

This novel DNA functionality creates the opportunity for the design and construction of a wide variety of simple and inexpensive biosensing applications. A previous study demonstrated triggered HCR where the product was a self-assembling, branched DNA nanostructure whose size grew exponentially by increasing the number of molecular species present [5]. Here we describe a DNA triggered HCR which forms a dendritic nanostructure that also grows exponentially, but which requires very few DNA hairpin strands. The minimal complexity of this system results in few sequence constraints, permitting the detection of arbitrary DNA sequences with minimal sequence redesign. In the absence of the target strand (T_1), the two hairpins (α and β) do not react and remain in closed form. However, when added, T_1 binds to and opens up a by toe-hold mediated strand displacement. Each opened hairpin can subsequently open and bind two copies of the other hairpin resulting in formation of the dendritic nanostructure (Fig. 1). As explained below, the target sequence for the first version of this system needed to have a repeated subsequence. The detection system was further modified for detection of any arbitrary target sequence (T_2) by introducing a third hairpin, γ (Fig. 2). The system was also tested for the detection of unique sequence identifiers of HIV (human immunodeficiency virus) [9] and *Chlamydia trachomatis* pathogens [10].

1.2 Design of the dendritic HCR system

The nucleotide sequences of α and β were designed manually by first denoting generic sub-sequences that could accommodate the appropriate secondary structures of the desired closed hairpin conformations and the open conformations necessary for forming the dendritic com-

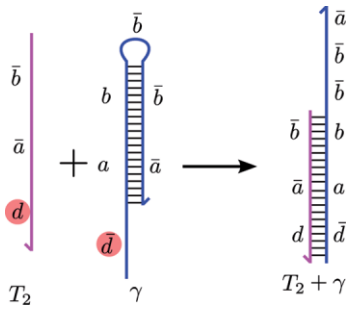

Figure 2. Detection of arbitrary target (T_2) using an adapter hairpin (γ). $T_2 + \gamma$ complex would open hairpin α, which would then trigger the dendrimer formation.

plex. In the first implementation of the detection system, the generic sub-sequence of α is a-b-b-c-$\bar{b}$-c-$\bar{b}$ and the generic sub-sequence of β is $\bar{b}$-$\bar{a}$-$\bar{b}$-$\bar{a}$-b-b-$\bar{c}$ (denoted from 5′-end to 3′-end with bar denoting sequence complementarity). Each strand forms a hairpin structure intended to have a bulged-loop protruding in the middle of the double-stranded region in addition to a single-stranded overhang (Fig. 1). The sub-sequences a, $\bar{a}$, c, and $\bar{c}$ are sufficiently short (seven residues) that when within a closed loop structure, they are unavailable for hybridization with their complements. Sub-sequences b and $\bar{b}$ are sufficiently long (15 residues) that their double-stranded stem structures are stable and do not allow the loops to open. The analyte, a target DNA strand, T_1, is a single-strand DNA oligonucleotide consisting of sub-sequences $\bar{b}$-$\bar{b}$-$\bar{a}$ having no stable secondary structure.

The actual nucleotide sequences represented by the sub-sequences were then designed by hand with careful attention paid to GC-content and the avoidance of unintended sequence repeats or reverse-complements. The predicted secondary structures of the initial sequence designs were evaluated using the MFOLD web server [11] which in most cases predicted the intended hairpin structure as the minimal energy configuration. The melting profile of the hairpins was experimentally determined and all the hairpins were found to be extremely stable with the melting temperature at around 70□C (data not included here). The more stable hairpin might reduce the overall rate of dendrimer formation because of the difficulty in opening through strand displacement. However, the thermal stability of the hairpins was crucial in order to avoid their spontaneous opening and resulting false positives.

Detection begins when annealed α and β hairpins are combined and then initiated with the addition of T_1. In the first step of the hybridization cascade, T_1 hybridizes with the single-stranded sub-sequence, a, of α and then by strand displacement, at both sub-sequences, b. The strand displacement results in an open-form bimolecular complex denoted $T_1 + \alpha$ (Fig. 1a).

In the second step of the hybridization cascade, the now single-stranded sub-sequences c-$\bar{b}$-c-$\bar{b}$ of the $T_1 + \alpha$ complex are available for hybridization to two copies of β by binding the single-stranded sub-sequence $\bar{c}$ on β. The hybridized copies of β then partially open via strand displacement and match their b sub-sequences with the $\bar{b}$ sub-sequences exposed in the $T_1 + \alpha$ complex. The resulting complex, $T_1 + \alpha + 2\beta$ (Fig. 1), constitutes the first layer of the nascent dendritic DNA nanostructure rooted by $T_1 + \alpha$.

The remaining metastable $\bar{b}$-$\bar{a}$-b stem-loop of β would, with at finite rate, spontaneously open and expose another copy of $\bar{a}$ (Fig. 1). In the open form, complex $T_1 + \alpha + 2\beta$ now has four $\bar{b}$-$\bar{a}$ sites available to hybridize the a-b subsequences in additional α strands. The reaction of the complex $T_1 + \alpha + 2\beta$ with four copies of α yields the new complex $T_1 + 5\alpha + 2\beta$, constituting the second layer of the growing dendritic nanostructure. The rate of spontaneous opening and exposure of the $\bar{a}$ sub-sequence is necessary for, and is a factor controlling the growth of the dendritic nanostructure, and can be tuned by altering the stability of the b-$\bar{b}$ hairpin through sequence changes. For example, the sub-sequence b closest to the 3′-end on α and the sub-sequence b closest to the 5′-end on β can be replaced with sub-sequence $\tilde{b}$ which is similar to b, but contains a small number (1-4) of sequence changes which introduce mismatched base-pairings in the $\tilde{b}$/$\bar{b}$ double helix. This alternative sequence would be expected to slightly destabilize the remaining stem-loop structures shown in complexes $T_1 + \alpha + 2\beta$ and $T_1 + 5\alpha + 2\beta$. In practice, such sequence modifications were found to be unnecessary in demonstrating the functionality of the detection system.

Strand displacement, stem-loop openings, and hybridization of eight additional copies of β form the third layer of the nanostructure (complex $T_1 + 5\alpha + 10\beta$, Fig. 1). Because each α and β strand can open and hybridize two additional strands, the dendritic nanostructure grows with kinetics that are, in principle, exponential. In practice, however, at some point steric constraints will begin to limit the exponential kinetics. In this initial sequence design the target strand had the repetitive sub-sequence, $\bar{b}$-$\bar{b}$-$\bar{a}$. The detection system can be made to accommodate a non-repeating, arbitrary target sequences lacking a stable secondary structure, by using an adapter DNA strand, γ (Fig. 2). An arbitrary analyte sequence, T_2, composed of the sub-sequences $\bar{b}$-$\bar{a}$-d opens the adapter, γ, to expose the sequence $\bar{b}$-$\bar{b}$-$\bar{a}$ which like T_1 can initiate the cascade of the same α and β strands as already described.

It is possible, but relatively unlikely, that after one copy of β is bound to $T_1 + \alpha$ complex via b-$\bar{c}$ subsequence, instead of another β hairpin binding to the growing complex, the already bound β extends the hybridized region to include adjacent b subsequence forming hybridized pair between b-b-$\bar{c}$ subsequence of β and c-$\bar{b}$-c-$\bar{b}$ subsequence of α, with a bulged loop c on α. This may give rise to a linearly growing nanostructure instead of an exponentially growing dendrimer. However, the probability of this occurring is limited especially during the early phase of dendritic growth for a number of reasons. The relative

Biotechnol. J. 2013, 8, 221–227

concentration of the hairpins is high in the beginning, which would favor intermolecular interactions thereby increasing the probability of binding two copies of β instead of one to $T_1 + \alpha$. Moreover, due to entropic considerations, it is more likely that the first copy of the β hairpin that binds to the $T_1 + \alpha$ complex, binds to the c-$\bar{b}$ subsequence at the 3′-end instead of the one in the middle of the strand, prohibiting the linearly growing structures. Even taking the small probability of formation of the linear structure into consideration, it is safe to assume that the resulting dendritic growth kinetics will be super-linear.

2 Materials and methods

2.1 DNA strands and sequences

The sequences of the DNA strands for various targets and the corresponding hairpins are included in the Supporting information. Synthetic oligonucleotides were purchased from Integrated DNA Technologies (Coralville, IA) in unpurified form and were purified using denaturing polyacrylamide gel electrophoresis (PAGE).

2.2 Sample preparation

The α and β hairpins were heated to 90°C at 1 μM concentration in water, and then annealed rapidly by leaving them on the bench-top. While annealing γ, the concentration was 0.2 μM. All the hairpins and the target strands were then mixed in 1× PBS (pH 7.4) containing 300 mM Na^+ and 10 mM $MgCl_2$ for a total volume of 5 μL. Final concentration of α and β was 0.2 μM, whereas that of γ (wherever applicable) and target was 0.04 μM. During target titration, the concentrations of α and β were kept constant, whereas the concentration of γ and T_2 was adjusted accordingly. The solution was then incubated at 25°C for 2 h followed by 10 h at 30°C. For the kinetics studies, the samples for different time points were started so as to have same stop time.

2.3 Polyacrylamide gel electrophoresis (PAGE)

Formation of the dendritic nanostructure was determined by 6% non-denaturing PAGE using gels containing desired amounts of acrylamide monomer (19:1, acrylamide:bisacrylamide) in 1× PBS. The sample was mixed in equal volume with tracking dye containing 1× PBS, 50% glycerol, and 0.2% each of bromophenol blue and xylene cyanol FF. The gels were run on a Hoefer SE-600 electrophoresis unit at 10 V/cm. The gels were then stained with ethidium bromide and imaged using an AlphaImager® (Alpha Innotech) gel documentation setup.

2.4 Fluorescence studies

Fluorescence data were obtained on a Cary Eclipse Fluorescence Spectrophotometer from Varian, with temperature controller set to 25°C. Excitation and emission wavelengths were 303 and 367 nm, respectively [12], with 4 nm bandwidths. Hairpins were annealed before use. For each experiment, 0.5 μM of hairpin α was added to 80 μL of the reaction buffer. After acquiring 2000 s of fluorescence data in three cuvettes, $2 \times T_1$ was added in the first cuvette and $0.5 \times T_1$ was added in the other two cuvettes. After 10 000 s, $1 \times \beta$ was added in the second cuvette and water was added in the other two cuvettes to balance the volume. The data acquisition was stopped after 20 000 s.

3 Results and discussion

There were four parameters which needed to be optimized – Mg^{++} concentration, temperature of incubation, concentration of the reactant hairpin species, and time of incubation. The reaction buffer being used was PBS (phosphate buffer saline, pH 7.4) with 300 mM Na^+. However, it was found out that Na^+ alone was not sufficient to achieve a high yield of the dendrimer. The buffer had to be supplemented with Mg^{++}, which is a more effective counterion. At low Mg^{++} concentration, the rate of reaction was very slow, whereas with very high Mg^{++}, the dendrimer was forming even in the absence of the target strand (false positive).

Similarly, the rate of reaction was slow at the room temperature. On the other hand, at elevated temperatures, though the rate of opening of the stem-loop structure of bound β was high, the probability of hairpins opening by themselves was high, again leading to false positive. The concentration of the reactant hairpins and the target to hairpin ratio was also a crucial factor. In any biosensing application, it is always desirable to detect as low a concentration of target as possible. However, at the fixed target concentration, lower amounts of hairpins would create smaller dendrimer. At higher hairpin concentration, it again led to false positives.

Since it was assumed that the growth of the dendritic nanostructure would stop only due to steric hindrance, the ratio of target to reactant hairpins was kept $1:(5\alpha + 5\beta)$. The concentration of the target T_1 was kept 40 nM. In case of target T_2, the concentration of T_2 and γ was kept 40 nM each. Consequently, the concentration of the α and β hairpins was 200 nM each. The optimum Mg^{++} concentration was determined to be 10 mM. Since the length of the toe-hold which opens up the first hairpin and triggers the dendrimer formation is seven bases only, the initial incubation temperature was maintained at 25°C. After incubating thus for 2 h, to facilitate the opening of stem-loop structure in β hairpins after they are

BIOtec visions
www.biotecvisions.com

bound to the dendrimer, the temperature was elevated to 30°C.

A kinetics study was performed with the target T_2 to determine the extent of dendrimer formation with respect to time. Supporting information, Fig. S1 shows a 6% non-denaturing PAGE analysis of the reaction mixture incubated for various time durations. The two fastest moving bands represent the unreacted hairpins as indicated. Higher order incremental structures ($T_1 + \alpha$, $T_1 + \alpha + \beta$, $T_1 + \alpha + 2\beta$, $T_1 + 2\alpha + 2\beta$, and so on) appear as slower moving bands. After the structures exceed a certain size limit, they are unable to enter the gel, and they remain in the well, thus demonstrating dendrimer formation. The yield can be qualitatively determined by comparing the intensity of the dendrimer in the well, as well as by comparing the unreacted γ hairpin. One target T_2 strand binds to one γ hairpin. The more target strand consumed, the lower is the intensity of the band corresponding to the γ hairpin, thus the higher is the reaction yield. The yield is significant after 5 h, though it keeps increasing through 12 h. The negative control does not show any dendrimer formation even after 12 h. The appearance of some slower moving bands in the negative control is explained below. Thus, the proposed system is considerably faster than the linear HCR demonstrated by Dirks and Pierce [7] which needed 24 h for completion.

Once the incubation parameters were optimized, both the targets T_1 and T_2 were tested along with the unique sequence identifiers of HIV and *C. trachomatis* pathogens [9, 10]. Each pathogen target strand had a different set of hairpins, including the adapter hairpin γ, unique to its sequence. It is evident from Fig. 3A that in the presence of the target, the dendrimer forms very well (lanes 1, 3, 5, and 7), whereas there is no dendrimer formation when there is no target (lanes 2, 4, 6, and 8). As mentioned earlier and indicated in Fig. 3, the bulky structure which does not enter the gel represents the dendrimer and the dark bands at the bottom of the gel in negative control lanes represent unreacted hairpins. The fastest moving band corresponds to the γ hairpin, whereas the second fastest moving band corresponds to the equal sized α and β hairpins. The presence of unreacted hairpins after 12 h of incubation demonstrates the limitation on the size of the dendrimer imposed by steric constraints. It is to be noted here that some higher order structures can be observed (leaks) and they appear consistently irrespective of the presence of target. However, there is no large dendrimer formed due to these structures as is evident from the negative control samples. Thus, these structures could not possibly have formed by spontaneous opening and hybridization of the hairpins without the target strand. It is possible, though, that these bands represent the homo-dimers and -trimers of the α and β hairpins as illustrated in Fig. 3B. These oligomeric structures must have formed while annealing the hairpins, and as can be predicted from the Fig. 3B, are quite stable, which is further corroborated from the gel image in Fig. 3A as the bands labeled leak. The formation of tetrameric and larger structures is hindered by steric factors as well as the high degree of stability of the individually folded hairpins. It is also to be noted here that the tendency to form such dimers and trimers is considerably less in case of γ hairpin because of its shorter size.

The mechanism of the dendrimer formation through hairpin opening and hybridization was further confirmed by fluorescence quenching. One of the adenine bases in the toe-hold region of α hairpin was replaced by its analog – 2-aminopurine (2AP, Fig. 4) [12]. 2AP is a fluorescent marker when unpaired. However, pairing with the thymine base quenches its fluorescent activity. Thus, when the target sequence T_1 opens the α hairpin, quench-

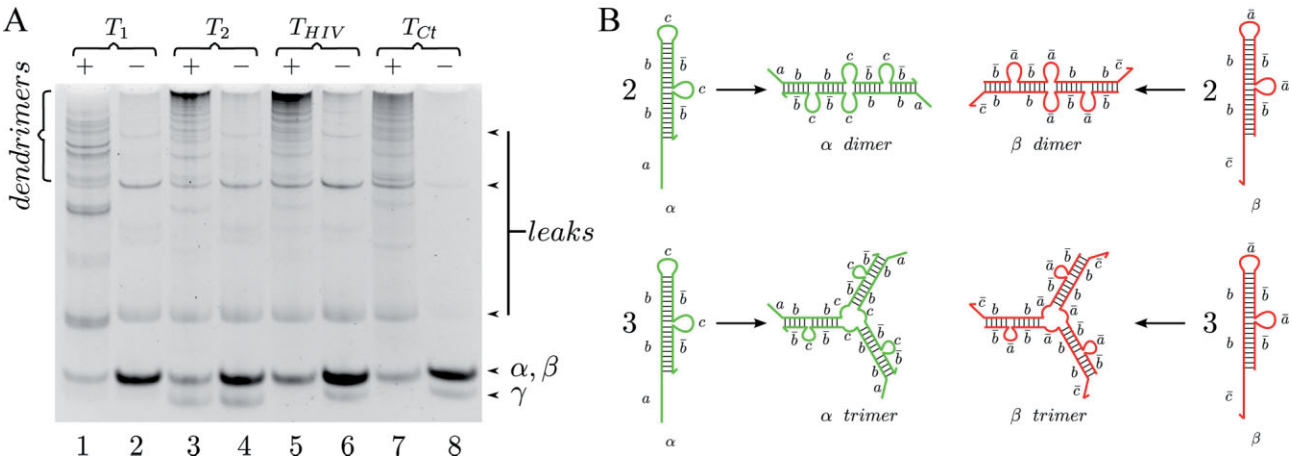

Figure 3. (**A**) Six percent non-denaturing polyacrylamide gel analyzing the detection of various targets through dendrimer formation. Samples in odd numbered lanes contain target, whereas samples in even numbered lanes are negative controls for the preceding sample. The order of the target sequences is: arbitrary target with repetitive subsequence (T_1, lanes 1 & 2); arbitrary target with non-repetitive subsequence (T_2, lanes 3 & 4); HIV target (lanes 5 & 6); *Chlamydia* target (lanes 7 & 8). (**B**) Proposed mechanism for the leak bands.

Biotechnol. J. 2013, 8, 221–227

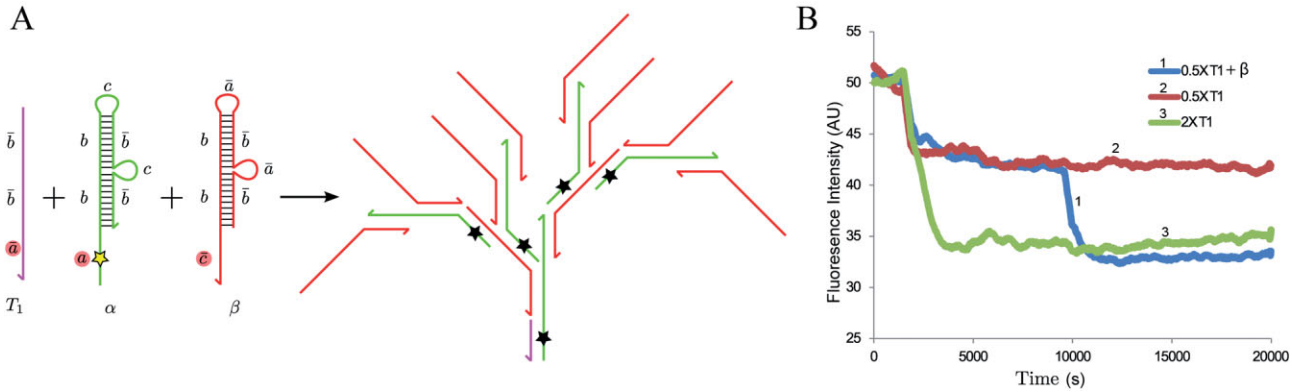

Figure 4. (**A**) An adenine base in the toe-hold region of α hairpin is substituted with its analog – 2-aminopurine which is a fluorophore. When target T_1 opens the hairpin, it quenches the fluorescence. Quenching would also occur when α binds to the unfolded β in the growing dendrimer. (**B**) Quenching of fluorescence is observed upon addition of T_1 and β. The fluorescence intensity is normalized for all the samples at time zero.

ing would be observed (Fig. 4). Similar quenching would be observed when the α hairpin would open upon binding to the dendritic nanostructure through opened β hairpin. This is experimentally corroborated in Fig. 4. Addition of excess target led to full quenching. When the target to α ratio was 1:2, the quenching was approximately halved. This proves that the target is binding to the α hairpin. Moreover, addition of β hairpin to the half-quenched solution led to full quenching, signifying that it first binds the T_1-α complex, which then further binds and opens the remaining α hairpin.

In the current set-up, the detection of dendrimer formation was done by non-denaturing PAGE. As illustrated in Fig. 3A, it was a good indicator of the detection and was able to detect approximately 200 fmol of the target. It would thus be interesting to determine the sensitivity of the system. Keeping the concentration of the reactant hairpins constant (200 nM α, 200 nM β, concentration of γ equal to that of the target), a range of concentrations were tried for the target strand T_2. It is evident from Fig. 5 that even though there is some dendritic nanostructure formation at the target concentration of 2 nM (10 fmol, lane 2, 1/100 ratio of target to each hairpin), the yield is sufficiently high for positive detection at the concentration of 10 nM (lane 4, 50 fmol).

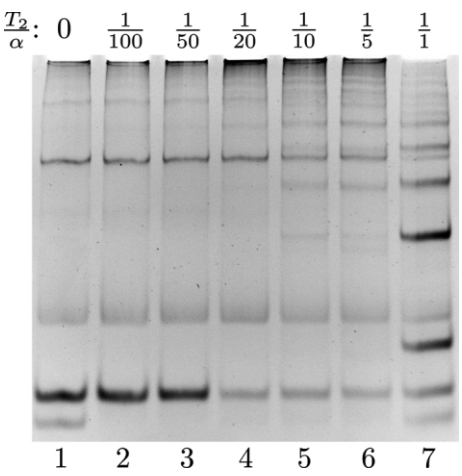

Figure 5. Six percent non-denaturing PAGE analysis of the dendrimer formation to determine the sensitivity of the system in detecting target T_2. Detection of as low as 10 nM (50 fmol) of target is possible (target to hairpins ratio = 1:1γ + 20α + 20β, fourth lane from left) using PAGE.

The obvious assumption in this experiment is that the lower amount of target strand would cause larger dendrimer formation owing to high hairpins to target ratio. However, as mentioned earlier, the size of the dendrimer is eventually limited by steric factors. This explains the significant amount of unreacted hairpins in lanes 2 and 3 in Fig. 5 corresponding to 1/100 and 1/50 target to hairpin ratio. Expectedly, at the target to hairpin ratio of 1/1 (lane 7), only smaller superstructures are formed with a distinct absence of dendrimer in the well. There are still some unreacted hairpins in this case, which could be due to the slower reaction kinetics of the dendritic HCR reaction with lower temperature incubation.

Apart from sensitivity, another important criterion to judge any biosensor is specificity. Specificity of the dendritic HCR was determined by mutating the target sequence T_2 in the $\bar{a}$ subsequence which opens the γ hairpin after binding to its toehold (Supporting information, Fig. S2). The mutation was achieved by substituting bases thus creating mismatches. Three different mutated strands were tried, with one, two, and three consecutive mismatches, respectively. Non-denaturing PAGE analysis showed that there was dendrimer formation in all the three cases (Supporting information, Fig. S2). This result demonstrates some looseness in the specificity of the system. However, it also demonstrates the robustness of the system which may be useful while dealing with mutated or evolving pathogen. It should also be noted that addition of an arbitrary strand with no sequence similarity to the target strand resulted in no dendrimer formation (data not shown).

4 Concluding remarks

The versatility of DNA has been described here when certain fundamental properties of DNA, such as strand displacement and hybridization through Watson–Crick base-pairing, have been exploited to create a biosensing system with signal amplification. It involved dendritic HCR where the presence of the target sequence triggered the formation of a dendritic nanostructure by opening the specially designed hairpin molecules. The growth of the dendrimer was designed to be at least super-linear and at best exponential. The system was tested for an arbitrary target sequence as well as unique sequence identifiers of HIV and *C. trachomatis* pathogens. In the absence of any target, there was predictably no dendrimer formation.

The exponential HCR detection strategy is not as sensitive as certain other electrochemical and piezoelectric biosensors, but it is relatively inexpensive. The detection can be performed by using non-denaturing PAGE and as low as 50 fmol of target can be convincingly detected. It should be possible to have an optical readout of the output of the dendritic HCR reaction. This can be achieved by using colloidal gold nanoparticles (AuNPs) and functionalizing them to bind to the dendrimer surface. AuNPs, when brought in close proximity, give a plasmonically induced color change as a result of collective electronic interactions [13]. Once colorimetric detection is incorporated, the dendritic HCR would offer an inexpensive and highly convenient alternative to other DNA based biosensors.

The authors would like to thank Peng Yin for helpful discussions regarding the research described here. Financial support was provided by NSF CCF-1141847, NSF EMT CCF-0829797: NSF EMT CCF-0829798, NSF-CCF 0829749, and AFSOR Contract FA9550-08-1-0188.

The authors declare no conflict of interest.

5 References

[1] Yurke, B., Turberfield, A. J., Mills, A. P. Jr., Simmel, F. C. et al., A DNA-fuelled molecular machine made of DNA. *Nature* 2000, *406*, 605–608.
[2] Omabegho, T., Sha, R., Seeman, N. C., A bipedal DNA Brownian motor with coordinated legs. *Science* 2009, *324*, 67–71.
[3] Tian, T., Mao, C., Molecular gears: A pair of DNA circles continuously rolls against each other. *J. Am. Chem. Soc.* 2004, *126*, 11410–11411.
[4] Sherman, W. B., Seeman, N. C., A precisely controlled DNA biped walking device. *Nano Lett.* 2004, *4*, 1203–1207.
[5] Yin, P., Choi, H. M. T., Calvert, C. R., Pierce, N. A., Programming biomolecular self-assembly pathways. *Nature* 2008, *451*, 318–322.
[6] Zhang, D. Y., Turberfield, A. J., Yurke, B., Winfree, E., Engineering entropy-driven reactions and networks catalyzed by DNA. *Science* 2007, *318*, 1121–1125.
[7] Dirks, R. M., Pierce, N. A., Triggered amplification by hybridization chain reaction. *Proc. Natl. Acad. Sci. USA.* 2004, *101*, 15275–15278.
[8] Green, S. J., Lubrich, D., Turberfield, A. J., DNA hairpins: Fuel for autonomous DNA devices. *Biophys. J.* 2006, *91*, 2966–2975.
[9] Cao, Y. C., Jin, R., Mirkin, C. A., Nanoparticles with Raman spectroscopic fingerprints for DNA and RNA detection. *Science* 2002, *297*, 1536–1540.
[10] Girjes, A. A., Carrick, F. N., Lavin, M. F., Single DNA sequence common to all chlamydial species employed for PCR detection of these organisms. *Res. Microbiol.* 1999, *150*, 483–489.
[11] Zuker, M., Mfold web server for nucleic acid folding and hybridization prediction. *Nucleic Acids Res.* 2003, *31*, 3406–3415.
[12] Rachofsky, E. L., Osman, R., Ross, J. B. A., Probing structure and dynamics of DNA with 2-aminopurine: Effects of local environment on fluorescence. *Biochemistry* 2001, *40*, 946–956.
[13] Mirkin, C. A., Letsinger, R. L., Mucic, R. C., Storhoff, J. J., A DNA-based method for rationally assembling nanoparticles into macroscopic materials. *Nature* 1996, *382*, 607–609.